

# A compliant, underactuated hand for robust manipulation

The International Journal of  
Robotics Research  
2014, Vol. 33(5) 736–752  
© The Author(s) 2014  
Reprints and permissions:  
[sagepub.co.uk/journalsPermissions.nav](http://sagepub.co.uk/journalsPermissions.nav)  
DOI: 10.1177/0278364913514466  
[ijr.sagepub.com](http://ijr.sagepub.com)



Lael U. Odhner<sup>1</sup>, Leif P. Jentoft<sup>2</sup>, Mark R. Claffee<sup>3</sup>, Nicholas Corson<sup>3</sup>,  
Yaroslav Tenzer<sup>2</sup>, Raymond R. Ma<sup>1</sup>, Martin Buehler<sup>3</sup>, Robert Kohout<sup>3</sup>,  
Robert D. Howe<sup>2</sup> and Aaron M. Dollar<sup>1</sup>

## Abstract

This paper introduces the iRobot-Harvard-Yale (iHY) Hand, an underactuated hand driven by five actuators that is capable of performing a wide range of grasping and in-hand repositioning tasks. This hand was designed to address the need for a durable, inexpensive, moderately dexterous hand suitable for use on mobile robots. The primary focus of this paper will be on the novel simplified design of the iHY Hand, which was developed by choosing a set of target tasks around which the hand was optimized. Particular emphasis is placed on the development of underactuated fingers that are capable of both firm power grasps and low-stiffness fingertip grasps using only the compliant mechanics of the fingers. Experimental results demonstrate successful grasping of a wide range of target objects, the stability of fingertip grasping, and the ability to adjust the force exerted on grasped objects using high-impedance actuators and underactuated fingers.

## Keywords

Adaptive, compliant, design and control, grasping, manipulation, mechanics, mechanism design, multifingered hands, robot, underactuated, underactuated robots, unstructured environments

## 1. Introduction

Building a robot to perform real-world tasks, such as bin picking, household chores, and disaster relief, requires robot hands that balance dexterity with robustness and cost. This trade-off is particularly important in realistic experimental scenarios, where the likelihood of an unexpected collision or a robot falling over is high. At the present time, many popular robot platforms for the end user are built with single-actuator parallel jaws, such as the Kuka YouBot (2013) or the Willow Garage PR2 (2013), or simplified multi-fingered hands optimized for power grasping configurations, such as Ulrich's UPenn/Barrett Hand (1988), the Robotiq Adaptive Gripper (2013), the Kinova Robotics Jaco (2013), and the Schunk Hand (2013). Highly articulated humanoid hands have been available for some time (e.g. Okada, 1979; Salisbury and Craig, 1982; Jacobsen et al., 1986; The Shadow Robot Company, 2013) and are undergoing continuous improvements in performance and durability (e.g. Schmitz et al., 2010; Bridgwater et al., 2012; Grebenstein et al., 2012). However, compared to their simpler counterparts, a relatively small number of dexterous hands are in use outside of the collaborations or institutions in which they were developed. Experience suggests that this disparity in user adoption is largely explained by the increased time, money, and expertise required for calibration, maintenance, and repair of more complex hardware.

This paper presents the iRobot-Harvard-Yale (iHY) Hand, shown in Figure 1, a hardened, medium-complexity robot hand designed to perform medium-dexterity manipulation tasks reliably in realistic experimental conditions. The goal in designing the iHY Hand was to achieve the reliability of a simple gripper, while also performing fingertip grasps, in-hand grasp transitions, and basic tool use tasks such as operating switches, triggers, and pliers. Rather than attempting to meet a general-purpose performance criterion for fine motor skills, such as in-hand manipulation, the iHY Hand was designed using a “bottom-up” approach, incorporating only those features needed to perform a library of specific task primitives. The SDM Hand (Dollar and Howe, 2010), a simple, single-actuator underactuated hand depicted in Figure 2, was chosen as an initial design concept, and was incrementally modified to add capability. The advantages of the SDM Hand architecture, such as durable, monolithic molded fingers and fully encapsulated sensor electronics, were preserved in the iHY Hand.

<sup>1</sup>Department of Mechanical Engineering and Materials Science, Yale University, USA

<sup>2</sup>School of Engineering and Applied Sciences, Harvard University, USA

<sup>3</sup>iRobot Corporation, USA

## Corresponding author:

Lael U. Odhner, Department of Mechanical Engineering and Materials Science, Yale University, New Haven, Connecticut, USA.  
Email: [lael.odhner@yale.edu](mailto:lael.odhner@yale.edu)



**Fig. 1.** The iRobot-Harvard-Yale (iHY) Hand is an underactuated hand capable of performing a wide range of tasks, including fingertip grasping and a set of dexterous manipulation primitives.

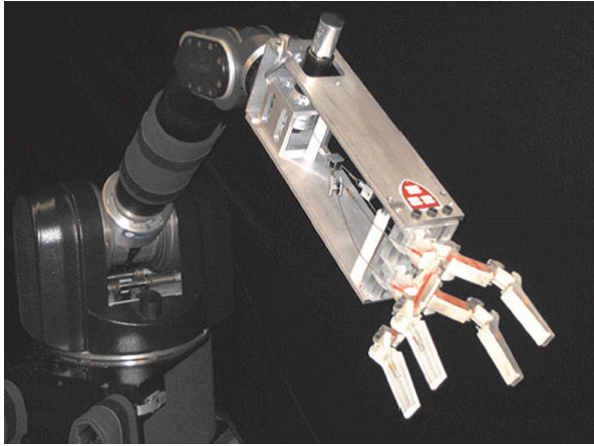


**Fig. 2.** The SDM Hand, a single-actuator underactuated hand, was designed to acquire enveloping grasps on objects of unknown size or position. It was used as the basis for the iRobot-Harvard-Yale (iHY) Hand design.

### 1.1. Simplified robot hands

The novel contributions of the iHY Hand must be placed in the context of the many simplified hands currently in existence. The most basic of these hands are designed for a single purpose, such as obtaining enveloping power grasps on a range of objects. Examples include Hirose's Soft Gripper (1978), Hanafusa and Asada's elastic-fingered gripper (1977), the UPenn/Barrett Hand (Ulrich et al., 1988), the SDM Hand (Dollar and Howe, 2010), and the Graspar Hand (Crisman et al., 1996). In these hands, the fingers or finger-like appendages are pre-positioned relative to the object to be grasped, and then the fingers are closed using one or several tendons. The passive behavior of the fingers causes them to wrap around the object without active

sensing or control. More exotic single-purpose hands have been designed, such as the MLab hand (Mason et al., 2012). This hand has only a single actuator that drives three fingers in parallel; the finger profiles are designed to passively acquire an object (whose shape is known *a priori*) in a specific orientation, despite high uncertainty in the object's initial pose.

Several robot hands are designed to perform multiple tasks through explicit decomposition of the actuated degrees of freedom. For instance, the Velvet Fingers Gripper combines a basic two-link, two-finger underactuated grasper with conveyor belt-like surfaces on the fingers (Tincani, 2012). The gripper actuator exerts internal forces on the grasped object, while the conveyor belt actuators can be used to rotate or position the object within the hand. Nagata (1994) and Bicchi and Marigo (2002) have also independently developed hands with actuated turntables at the fingertips of parallel-jaw grippers, providing a directly controllable degree of freedom (DOF) with the object in a secure grasp. Similarly, the Second Hand is designed to have a completely modular actuation system, so that each actuator imposes an independent synergy, that is, a coupled force or motion on all the joints of the hand (Grioli et al., 2012). These synergies can be customized to fit a user-specified set of tasks.

Hands using mechanical mechanisms to achieve multiple designed-in behaviors have also been developed; for example, those that can function as parallel jaw grippers or pincers when only the fingertips are used, and act as adaptive graspers when an object is placed in the center of the hand (Birglen et al., 2002; Ciocarlie et al., 2013; Kinova Robotics, 2013; Robotiq, 2013). In these hands, multiple modes of operation are accomplished using clever mechanical features, such as joint travel limits or unactuated tendons. Grasping with fingers in the direction of joint singularities can be used to obtain stiff lateral grasps (Birglen et al., 2008; Robotiq, 2013). The use of quasi-passive features such as brakes has also been implemented in underactuated manipulators to achieve a wider range of functionality (Arai and Tachi, 1991; Roy and Asada, 2009). For example, the SRI Hand utilizes selective braking with integrated dielectric elastomer joints to obtain fingertip and power grasps, and also to control brake transitions so that the object can be passively repositioned within the hand (Aukes et al., 2012). However, making the fingers rigid in order to achieve fingertip grasps is not always desirable. The iHY Hand uses careful parameter selection during the design phase to ensure that both power grasps and fingertip grasps exhibit appropriate compliant behavior, using only a single actuator per finger. Whether initial contact is made with a grasped object on the proximal links or the distal links, the iHY fingers can adapt to the object's contours without accurate sensing information. This new approach simplifies the finger design, as no additional mechanisms or components are needed, and also enables the use of

non-backdriveable tendon actuators without sacrificing the ability to produce low-impedance fingertip behavior.

In addition to demonstrating new design concepts for the mechanics of underactuated grasping, the iHY Hand is built to improve upon the state of the art in hand cost, durability, and maintainability. Similar to the SDM Hand, the fingers of the iHY Hand are sealed, monolithic polymer parts that can be easily attached to or removed from the hand in a modular fashion. Breakaway joints and compliant flexure joints minimize damage from accidental impacts. Lastly, the proprioceptive and tactile sensors in the iHY Hand are built entirely from commercial, off-the-shelf integrated circuits, keeping the overall cost of the hand low (approximately US\$5000).

## 1.2. Overview

We begin with an analysis of the range of tasks that the iHY Hand is designed to perform, followed by presentation of the hand design itself. Section 3 analyzes how the design of the fingers was tuned to be passively adaptive in both caging and fingertip grasps. Experimental results in Section 4 link the performance of specific tasks to the mechanical features incorporated into the design of the hand.

## 2. Hand design

The iHY Hand was constructed as part of the DARPA Autonomous Robotic Manipulation-Hardware program (ARM-H), which greatly influenced the design process. The evaluation of prototypes in ARM-H was strictly experimental. A set of challenge tasks was provided to all program participants, and these challenge tasks determined the functional requirements of the hand. We chose to approach the design process from the bottom up, starting with the very simple SDM Hand, an underactuated hand having flexure-based fingers shown in Figure 2. The SDM Hand, while extremely durable, was designed entirely around the ability to acquire a stable enveloping grasp on unknown objects. This design was modified to encompass the wider range of tasks specified by ARM-H, adding as few components as possible to obtain the desired capability. There was little concern that the hand be capable of general-purpose use in any currently understood sense (see, for example, those discussed by Okamura et al., 2000); nor was the design analyzed within the typical framework of workspace analysis or Jacobian-based performance indices, such as a conditioning metric (Salisbury and Craig, 1982) or a determinant-based metric (Yoshikawa, 1985). Instead, the hand and finger design parameters were analyzed by breaking down each of the desired challenge tasks into primitive operations, whose behavior was designed into the passive mechanics of the hand. This section describes the tasks that the iHY Hand was designed to perform, and overviews the major hand subsystems.

### 2.1. Functional requirements

The representative set of tasks that the iHY Hand was chosen to perform were drawn from a broad range of common scenarios. Existing studies on Activities of Daily Living were consulted in initial ideation (Cutkosky, 1989; Matheus and Dollar, 2010), but the final list of tasks to be performed was set by the ARM-H program in consultation with all of the participating research groups:

- pick up a key and put it into a lock, then unlock and open a door;
- open a zipper on a backpack and remove the contents;
- pick up a pair of wire cutters and cut a wire;
- pick up and write with a whiteboard marker;
- grasp a radio handset and activate the push-to-talk button;
- grasp a drill and use it to drill a hole;
- grasp and turn on a flashlight from an unknown initial pose;
- grasp a hammer in a fashion suitable for use from an unknown pose;
- grasp and move a heavy, unknown object such as a rock or cinder block.

Interestingly, this list overlaps with evaluation criteria used for prosthetic hands (Resnik et al., 2013); both focus on access (locks, doors, or zippers) and basic tool use (hammers, drills, wire cutters, flashlights, etc.). Each evaluation task was analyzed to determine possible strategies for execution using as few actuators as possible. Bench-level prototypes, constructed using Shape Deposition Manufacturing (Merz et al., 1994) and three-dimensional (3D) printing, were used to evaluate these strategies, and simplified analytical models were used to identify the critical parameters of each task.

Initial experimentation and analysis produced a set of primitive grasping and manipulation operations that could be used in some sequence to perform all of the challenge tasks. Figure 3 illustrates the grasp modalities chosen. It is worth mentioning here that the names of the grasps mirror those found in human grasp taxonomies, but are used here mainly to indicate the location and number of contacts between the hand and the object. The objective was the performance of some task, rather than a reproduction of the human approach. This can be clearly seen in the lateral grasp shown in Figure 3(b), which mimics the human lateral grasp only in that one finger is used to hold an object against the side of the others. The principal functionality that was kept from the SDM Hand is the cylindrical power grasp, in which the fingers are interlaced around a roughly cylindrical object. All of the other grasps in the set chosen required incremental modifications of the SDM Hand design. Most importantly, fingertip grasps, shown in Figure 3(a), were needed for picking up small objects, but also for acquiring initial grasps on larger objects, especially if these were acquired from the surface of a table where a power grasp could not be directly acquired.

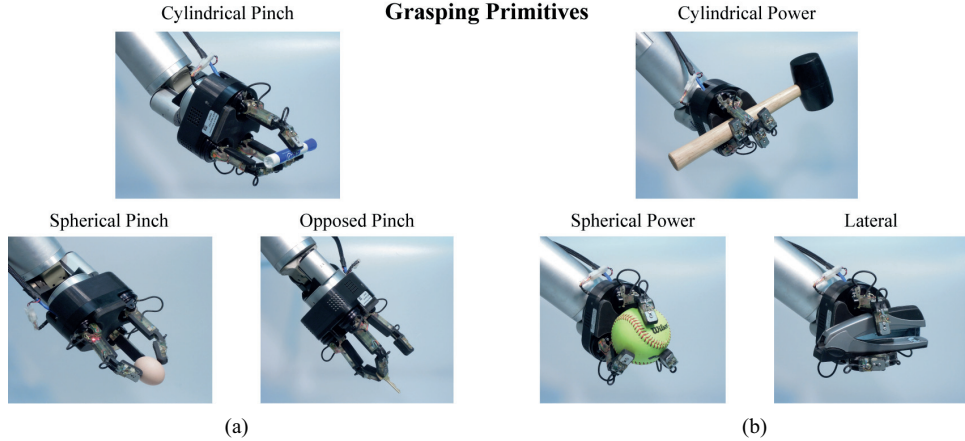


**Fig. 3.** The set of passive adaptive grasps that the iRobot-Harvard-Yale (iHY) Hand was designed to perform is shown above, including cylindrical, spherical, and opposed pinch grasps, as well as cylindrical and spherical power grasps. The lateral grasp (bottom right in (b)) is performed by rotating two fingers so that they are normal to the plane of finger motion, providing a stiff surface against which the third finger can push.

A small set of manipulation primitives necessary to perform the challenge tasks were also identified, and are depicted in Figure 4. Again, these were not intended to be anthropomorphic operations, nor were they intended to enable general-purpose in-hand manipulation (such as gaited manipulation). The most useful primitives for in-hand repositioning of grasped objects were found to be shifting from one grasp type to another, such as transitioning from a pinch grasp to a power grasp (shown in Figure 4(a)), or in adjusting the orientation of the object relative to the finger contact points. For instance, picking up a key in an opposed pinch grasp and putting it into a lock often entails reorienting the key into a pinched configuration between the fingers (Figure 4(c)), then rotating the key so that the blade is aligned with the axis of the lock (Figure 4(b)), as in Rus (1992). Button-pushing tasks are important to using many common tools, such as drills, so the ability to perform a reversible single-fingertip squeezing motion (Figure 4(d)) was also required.

## 2.2. Critical failure modes

In addition to the functional requirements imposed by the ARM-H challenge tasks, feedback from researchers using commercial robot hands was used to articulate a set of failure modes to be avoided in the iHY Hand. The principal failure mode considered was damage due to collision. In unstructured environments, errors in perception or control can result in unintended “crashes” between the hand and the environment. It is important that hands be able to survive such events, both for eventual applications outside the lab and for fast experimental development; researchers can test ideas more quickly when mistakes do not result in hardware damage that is expensive or slow to repair. Although active impedance control can be used to provide such robustness, passive compliance is typically less expensive and more

reliable if impacts are sudden, or if power to the hand is lost.

Thermal management was also found to be a key concern for users of robot hands. Because finger motors must be compact, they are often driven at or near their peak capability during normal use. As a result, these motors often overheat, limiting the duration of experiments. Although adaptive features such as automatic current-limiting controllers can be used, these can lead to repeatability problems in hot environmental conditions, or when the hand sees continuous use. The goal for the iHY hand was to design the hand mechanics and transmission so that the actuators never exceed their continuous-duty rating.

## 2.3. Hand structure and actuation

The design of the iHY Hand began with the SDM Hand, preserving mainly the structure and fabrication of the two-link underactuated fingers. Instead of four fingers coupled by a differential transmission, three fingers each having a single flexor tendon were used. The three-fingered design was chosen to adhere to the bottom-up philosophy, as it provides a minimal basis for accomplishing the grasping and manipulation primitives making up the challenge tasks. For example, at least three fingers are needed to obtain spherical grasps on objects, or to grasp cylindrical objects with interlaced fingers. Trigger tasks, in which one finger is squeezed on an already-grasped object, were found to be much easier with three fingers, so that two could be held fixed during the process. The most complex manipulation operation, finger pivoting (shown in Figure 4(b)), was also found to require three fingers: two opposed fingers to hold an object, and the third finger oriented perpendicular to push the object.

The fingers are mounted to the palm in a triangular pattern, depicted in Figure 5, so that a pair of fingers sits in opposition to a third finger, hereafter called the thumb. The

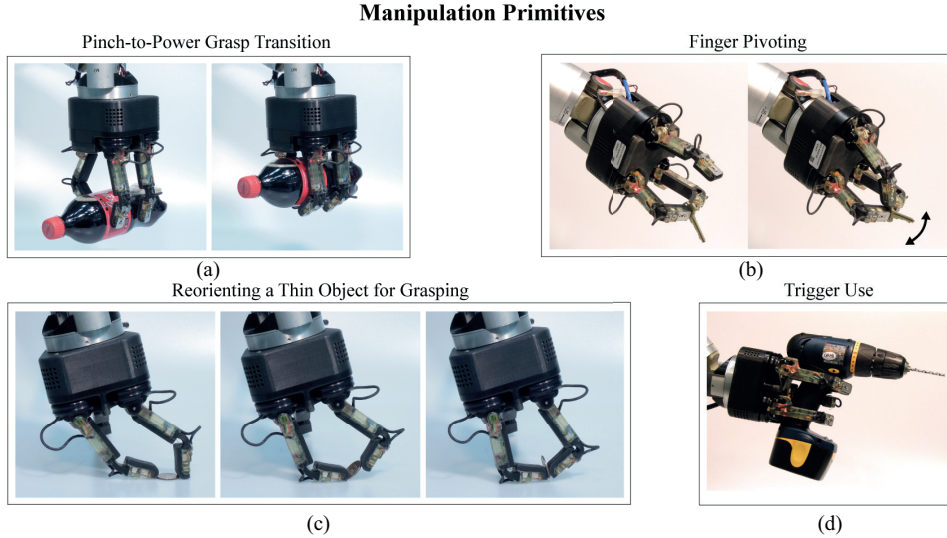


**Fig. 4.** Several manipulation primitives were identified from the list of required tasks. Among these, the most important were the ability to transfer an object from a pinch grasp securely into a power grasp (a), the process of rotating a thin object such as a key to acquire a power grasp (c), the ability to pivot an object grasped between two fingers using the third (b), and the usage of simple triggers and buttons (d).

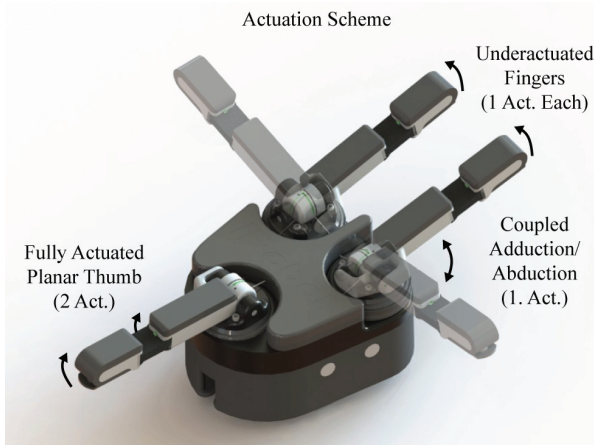


**Fig. 5.** A total of five actuators are used in the iRobot-Harvard-Yale (iHY) Hand: each finger has an identical actuator controlling finger flexion. The thumb has an additional tendon so that the position of the thumb in the plane can be controlled. The two underactuated fingers have a coupled adduction/abduction motion to switch from cylindrical, spherical, and opposed grasps.

finger pair is actuated to adduct and abduct in a coupled fashion, so the fingers can be rotated between an opposed configuration, a spherical configuration meeting at a point in the center of the hand workspace, and an interlaced configuration suitable for grasping cylindrical objects. In this way, the finger/palm layout is similar to the Schunk Hand or the Barrett Hand.

The number and kind of actuators used on the hand were identified as major drivers of cost and performance. Direct current (DC) motors (EC-20, Maxon Motor AG, Sachseln, Switzerland) were used, connected to a non-backdriveable worm gear transmission. The choice of a

worm gear transmission was related to the problem of thermal overload. Although backdriveable transmissions, such as planetary gears, provide low impedance actuation, they also require that the torque to hold the fingers in place at steady state be actively produced, rather than passively produced through friction. This greatly increases the power dissipated at steady state inside the hand enclosure. In contrast, the actuators on the iHY Hand are constructed so that once a grasp is acquired, minimal current is needed to actively resist any disturbance force on the tendons. With only a small cooling fan in the wrist enclosure, the iHY Hand can hold any desired pose almost indefinitely. Section 3.2 discusses how the passive mechanics of the hands were modified to allow low-impedance fingertip forces despite the use of high-impedance actuators.

The iHY Hand has five actuators: each of the three fingers has a single flexor tendon running the length of the finger, and the adduction/abduction DOF on the finger pair is driven by a fourth. A fifth actuator powers an extensor tendon on the proximal joint of the thumb. This actuator allows the link angle of the thumb proximal and distal joints to be set independently, and is particularly useful for tasks in which the tip of the thumb needs to move arbitrarily in the plane, such as the finger pivoting shown in Figure 4(c). Because the extensor tendon has no antagonistic return tendon, it can be slackened so that the three fingers function identically. The entire hand weighs 1.35 kg, and the palm assembly housing the actuators fits into a package only 82 mm from the wrist to the palm surface. This is comparable to available commercial robot hands, such as the Barrett Hand. The total of five actuators places the hand in the middle of the range of the robotic hands available for research and prosthetic

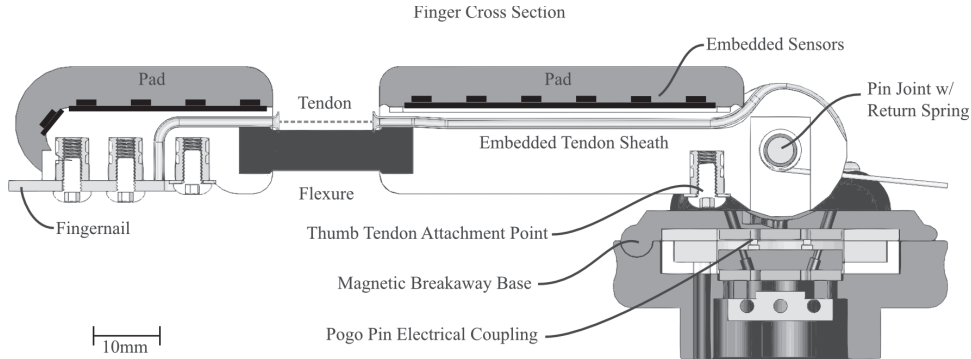


**Fig. 6.** Cross-section view of the iRobot-Harvard-Yale (iHY) finger design, showing the components embedded in the molded monolithic finger.

applications, well below most general-purpose research hands but above most underactuated grippers (Belter et al., 2013).

#### 2.4. Finger design

The iHY fingers, depicted in Figure 6, utilize a two-link modular design similar to its precursor, the SDM Hand shown in Figure 2. The proximal pin joint connecting the finger to the hand is mounted on a circular magnetic base (also shown in Figure 6), which serves as a modular attachment point, and also as a high-force breakaway coupling to ensure that fingers will be minimally damaged in a catastrophic collision. Spring-loaded “pogo pin” electrical contacts further simplify the modular fingers so that replacing a finger can be accomplished by snapping the finger in place, then attaching the flexor tendon. A tendon attachment point for the antagonistic tendon used on the thumb is included at the base of the proximal link on all fingers, so that any finger can be interchangeably used in any position on the hand.

The fingers were constructed using a casting and over-molding process based on Shape Deposition Manufacturing (Merz et al., 1994; Cham et al., 1999; Dollar and Howe, 2006), but streamlined for higher-volume production by the elimination of intermediate machining steps. The various internal components of each finger (circuit boards, sensors, wiring, and cable guides) were inserted into a mold cavity. Elastomeric parts, such as finger pads and flexure joints, were pre-molded in separate cavities and inserted along with the other components. A glass-filled epoxy resin was then injected into the mold, forming a single monolithic part. Figure 6 depicts a cross-section of the iHY finger. Like the SDM Hand, the distal joint of each finger is an elastomer flexure. A more conventional pin joint with an in-molded bushing was chosen for the proximal finger joint. Because the fingers are monolithic parts without seams or fasteners, they can resist water, dirt, and impact.

One of the more important features of the iHY finger is its high compliance, especially at the distal flexure. The distal flexure hinge admits out-of-plane motion, illustrated in

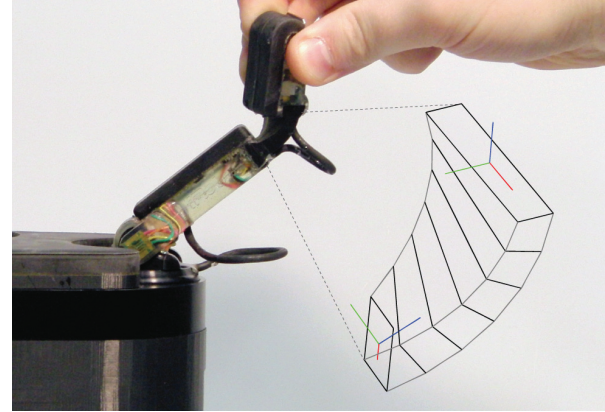


**Fig. 7.** The compliant flexure joints on the iRobot-Harvard-Yale (iHY) fingers allow three-dimensional fingertip motion.

Figure 7. The proximal pin joint includes a torsion spring, which provides the proximal joint with some elasticity. This compliance serves several purposes: firstly, because the fingers do not have extensor tendons, the joint elasticity alone extends the fingers when the flexor tendons are relaxed. This is particularly useful when operating the hand in an unknown environment where collision with obstacles is likely, so that fingers merely deform in response to unplanned contact. The torsional compliance at the distal flexure joint provides a similar robustness to the fingertips for out-of-plane contact. The second purpose served by passive finger compliance is passive adaptation to the shape of the object grasped, which removes the need to detect and react to small variations in surface geometry.

The addition of a fingernail on the distal link of each finger proved to be a useful and inexpensive feature on the iHY Hand. When grasping small objects, or sliding a finger along the surface of a table, the hard, smooth end of the nail served both to provide a repeatable point of contact at the fingertip and to passively align the finger against the table, like a spatula pressed against a griddle. To allow for varying nail length, mounting screws were used to fasten the removable nail onto the fingertip.

## 2.5. Sensing

The iHY Hand's sensor system, diagrammed in Figure 8, consists of tactile arrays covering the fingers and palm, flexure deformation sensors in each distal finger joint, magnetic encoders at each proximal finger joint, and accelerometers in the distal finger links. The sensor suite measures the hand configuration, and also provides contact detection/localization. Wherever possible, commercial, off-the-shelf parts were used to maximize the reliability and minimize the cost of the hand. Two of the sensors developed for the hand are novel: sensors for detecting the 3D deformation of the distal flexure joints (Figure 7), and inexpensive microelectromechanical system (MEMS) tactile arrays for localizing the contact of objects with the hand.

Flexure deformation can be used to obtain important information about contact detection (Jentoft and Howe, 2011), object localization, and measuring forces (Jentoft and Howe, 2012). However, no suitable large-deformation, multi-DOF flexure sensor exists, so a new sensor was created. This sensor measures the local curvature at two points on each end of the joint, using four modules that measure the local angle using optical fiber shining onto a pair of surface-mounted phototransistors. The four local curvature measurements are fit by linear regression to determine an approximate interpolated bending profile for the “backbone” of the bending flexure. The backbone curve is then numerically integrated along the length of the joint. This sensor makes it possible to evaluate joint flexion, twist, combination of these, and shear. Greater accuracy can be obtained by combining this four-point bending measurement with the measured tendon excursion and the accelerometer embedded in the fingertip.

The iHY tactile arrays used commercial off-the-shelf MEMS barometers (MPL115A2, Freescale Semiconductor, Austin, Texas) to provide tactile sensing with 10 mN sensitivity and 4.9 N range by casting the sensor circuit boards inside the molds for the fingers and palm, so that the rubber pads are firmly bonded to the sensors (Tenzer et al., 2012). Embedding the barometers, soldered onto standard surface-mount boards, solves the systems integration problem that has hampered use of tactile sensors in hand designs (Bicchi and Kumar, 2000; Dahiya et al., 2007). These are laid out in a  $2 \times 6$  array on proximal links, a  $2 \times 5$  array on distal links (with two wrapped around the fingertip), and a pattern of 48 on the palm concentrated in areas where contact is most likely, such as the edges of the palm (Figure 7). Tactile data on all sensors is available at 50 Hz through the data bus running along each finger into the palm.

## 3. Compliant underactuated fingers

So far, the design goals of the iHY Hand have been articulated, based on a set of grasping and manipulation challenge tasks set forth in the DARPA ARM-H program. The major subsystems of the hand have been presented, including the overall hand topology, the actuator and sensor subsystems,

and the fingers. This section explains how the underactuated iHY fingers were designed so that the passive adaptability of the fingers was useful not only in power grasping, but also in cases where only fingertip contact with an object is made. In keeping with the philosophy of minimal, incremental modification, this was accomplished by re-tuning the design parameters of the original SDM Hand, such as joint stiffness and link length ratio, rather than adding new mechanisms to obtain greater functionality. The fingertip force and stiffness properties are measured to demonstrate the typical behavior of the new fingers in power and fingertip grasping.

### 3.1. Designing compliant fingers for robust power grasps

The process of obtaining a power grasp with two-link underactuated fingers is illustrated in Figure 9. First, the fingers sweep in around the object. In order to maximize the chance of enveloping an object, the fingers must remain straight during this phase of motion. Once the fingers have contacted the object, the distal finger links must then cage around the object in order to complete the grasp. A variety of mechanisms have been used to achieve this behavior with a single actuator per finger. These include travel limits that cause the fingers to act as a single rigid link when straightened (Birglen et al., 2008), brakes in the joints, which must be switched off when contact is detected (Arai and Tachi, 1991; Takaki and Omata, 2006; Begoc et al., 2007; Aukes et al., 2012), as well as friction clutches that move only when the force on the finger tendon exceeds some threshold, as in the Barrett Hand and others (Ulrich et al., 1988; Saliba and de Silva, 1991; Chu et al., 2008). However, brakes and clutches increase the mechanical complexity of the finger, and all of these mechanisms also tend to stiffen the entire finger so that the passive fingertip compliance is eliminated, rather than allowing for some adaptive behavior. Although a friction clutch is mechanically simpler, it cannot be moved reversibly. Once a clutched finger has begun caging, only a complete extension of the finger will reset the clutch mechanism to its extended position, causing problems for some controllers and planners. Instead of relying on these mechanisms, an underactuated elastic design was used, similar to the Graspar and SDM Hands. Because these fingers have fewer actuators than phalanges, the actuator position or angle only partially constrains the configuration of the finger. The free motion of the finger can only be fully determined when considering the conditions for equilibrium in the finger (Quenouelle and Gosselin, 2009; Dollar and Howe, 2010). The SDM Hand achieved this sweeping motion by designing the distal finger joints to be four to five times stiffer than the proximal joints, as analyzed by Dollar and Howe (2010). The iHY Hand used the same passive joint stiffness ratio as the SDM Hand in order to preserve this desirable behavior.

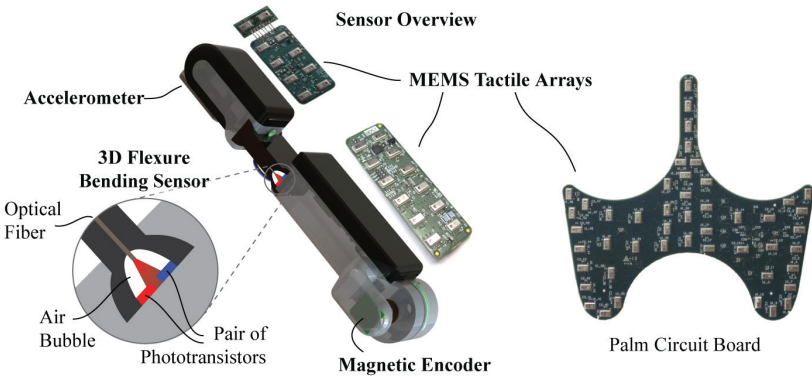


**Fig. 8.** Each finger contains joint angle sensing via a magnetic encoder, optical flexure bending sensor, and an accelerometer. Tactile sensing is provided by an array of microelectromechanical system (MEMS) pressure sensors.

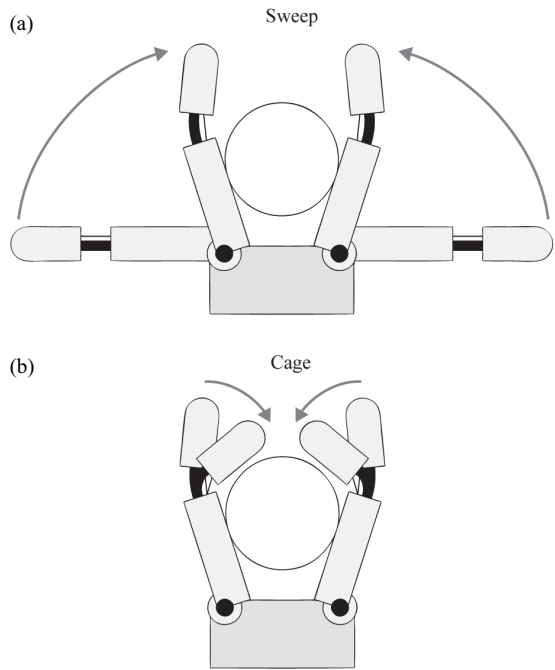


**Fig. 9.** The process of acquiring a power grasp can be divided into approximately two phases: the sweeping phase, in which the proximal finger links are brought into contact with the object, and the caging phase, in which the distal links flex to encircle the grasped object.

The compliant behavior of the iHY finger during sweeping and caging can be understood by considering the simplified model shown at the bottom of Figure 10, consisting of a spring-loaded four-bar linkage in which the tendon serves as the fourth link running parallel to the proximal joint. A more accurate model for the iHY finger, also shown in Figure 10, would include several higher bending modes of the distal flexure joint as described by Odhner and Dollar (2012), and a whole-finger model is described in detail by Odhner et al. (2012). For both of these models, the motion

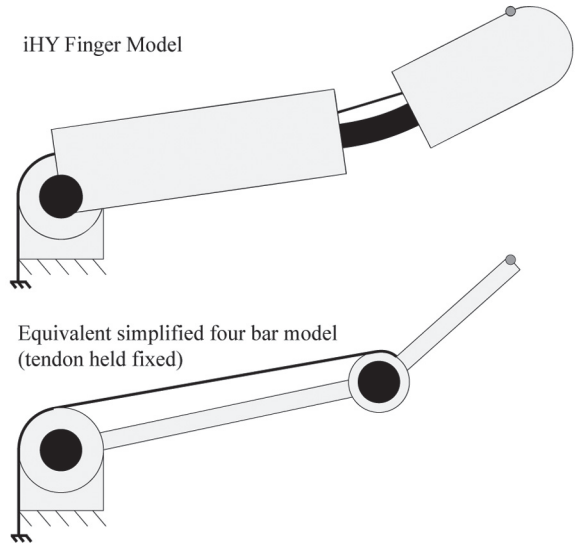


**Fig. 10.** The iRobot-Harvard-Yale (iHY) fingers were modeled as two-link underactuated mechanisms by constraining the total tendon length on the proximal and distal joints, while allowing the joints to deform elastically. This model was used to approximate finger compliance on the proximal and distal links.

of the fingers during the sweeping phase of grasping can be modeled by treating the length of the flexor tendon as a rigid constraint on the system, then by minimizing the elastic energy in the two joints to find the equilibrium finger configuration as the finger closes. Once a single contact has been made and the fingers start caging, the underactuated finger acts as a differential transmission, exerting a torque on each of the finger links proportional to the moment arm of the tendon at each joint. Thus, the force on the proximal finger links will increase gradually as torque builds up on the elastic distal joint. Once the hand has closed around the object, the fingers are no longer underactuated in the sense that their motion is fully constrained by multiple contacts with the grasped object. Due to higher-order elastic

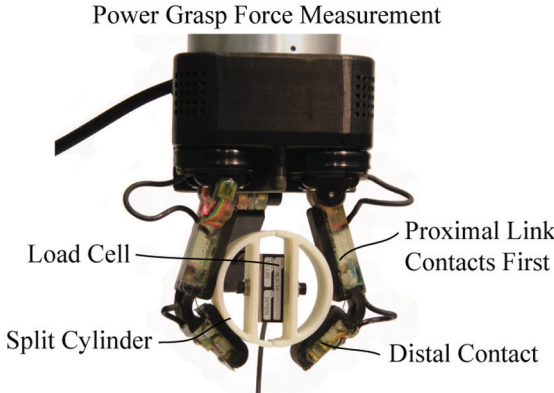


**Fig. 11.** An apparatus for measuring the internal force on an object in a power grasp configuration.

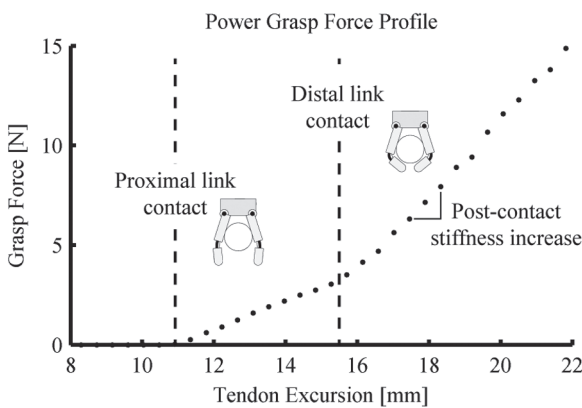


**Fig. 12.** Power grasp force on a 65 mm wide object as tendons are tightened. The “knee” in the curve corresponds to the point at which the distal links make contact with the object, stiffening the whole hand.

deformations, such as the rubber finger pads and the internal deformation modes in the flexure joint, the power grasp will not be infinitely stiff, but it will be sufficient to hold even heavy objects.

The contact forces on a grasped object were measured in a simple experiment to illustrate the changes in the iHY finger mechanics as a grasp is acquired. This was accomplished by constructing a cylindrical object split down the middle, having a load cell embedded in it as depicted in Figure 11. The underactuated fingers were moved into an opposed, planar configuration, and closed slowly on the grasped object. The load cell measured the force exerted between the two fingers in the direction of the split, which was oriented such that it was symmetric with the fingers, as shown in Figure 11. The results, plotted in Figure 12, confirm that the internal forces on the object in the direction of the split remain low (<3 N) until the caging process is complete. After this point, further excursion of the tendons causes a linear increase in internal force, to the point measured.

The underactuated behavior of the finger can be clearly seen in the changing slope of the force–excursion curve in Figure 12 as the fingers close. In the caging phase, the mechanism is underconstrained, and consequently force builds up slowly due to bending of the flexure. After the distal links have also made contact, the whole hand mechanism is stiffened by the added constraints, so much larger forces can be exerted on the object. In addition, because the caging motion is reversible except for a small amount of viscoelastic hysteresis in the flexure joint, tasks in which trigger-like motions are needed (operating a power drill, for example, or depressing a button on a radio handset) are accomplished without specialized mechanisms or control functions. Finally, it is important to remember that although the forces measured in this experiment are small, the fingers can resist much larger forces than they can actively exert due to the non-backdriveable tendon actuators. For example, the video in Multimedia Extension 1 (at 3:08) depicts the iHY Hand picking up a 22 kg weight in a cylindrical power grasp.

### 3.2. Extending compliance to stable fingertip grasps

Like power grasping, fingertip grasping and manipulation tasks also place requirements on finger compliance. In order to apply predictably low forces and adapt to the shape of grasped objects, compliance should be high in the direction normal to fingertip contact, as illustrated in Figure 13. In addition, fingers must also be stiff in the shearing directions to provide stable pinch grasps. Finally, fingers must be robust to collision with rigid surfaces because many objects acquired via fingertip grasps are initially resting on rigid surfaces. Meeting these compliance requirements with an underactuated finger is particularly difficult due to the intrinsic compliance of the finger mechanism and the limited number of actuators. For example, the four-bar linkage formed by the simplified model in Figure 10 will move passively in one direction even if the tendon is locked. Attempts at obtaining stable fingertip grasps with underactuated fingers have typically involved the addition of special-purpose mechanisms for stabilizing the fingertips, such as active locking mechanisms to reduce underactuated degrees of freedom as in the SRI Hand (Aukes et al., 2012) or in Begoc et al. (2007), specially designed fingertips to cup grasped objects as developed by Kragten et al. (2011), or strategically placed hard travel limits so that the fingers stiffen when moved into a pinching configuration, such as those found on the MARS and SARAH Hands (Birglen et al., 2008) or the Robotiq Gripper (2013). Fully actuated hands must solve the opposite problem: introducing compliance in order to achieve low-impedance fingertip contact. One way to do this is through series elastic actuation (Pratt and Williamson, 1995). The DLR Hand Arm System (Grebenstein et al., 2012) is a good contemporary

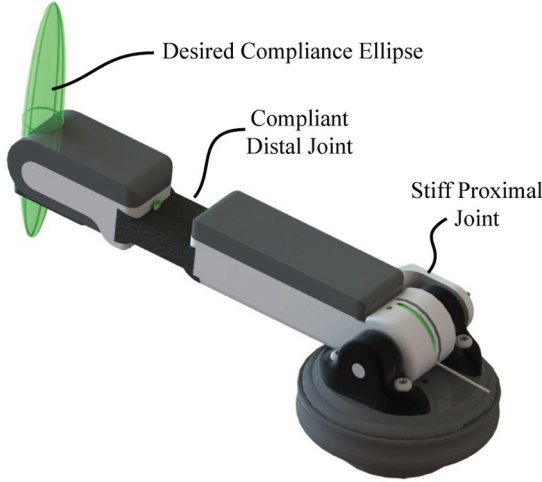


**Fig. 13.** The desired fingertip compliance ellipse is narrow in directions representing shear motion, and long in the direction representing normal motion. This means the finger will be able to move gently while still holding objects in a stiff grasp.

example, having variable stiffness drives that determine the elasticity of actuation at each joint.

Good fingertip grasping performance is achieved with the iHY Hand without adding any actuators, brakes, clutches, or hard stops to the design of the original SDM finger. Instead, the unavoidable compliance of the underactuated finger is tuned so that the finger's principal direction of compliance is favorable for grasping, acting almost like a series elastic actuator placed normal to the each fingertip. This aspect of the iHY finger design is the most important illustration of bottom-up philosophy in this work, because it shows how the incremental addition of functionality need not increase a hand's complexity.

As Figure 13 shows, the design goal of the iHY fingertips was to place the direction of principal underactuated compliance normal to the tips of the fingers. This was accomplished by analyzing the variation of the finger compliance over the whole distal link. Based on the flexure-based finger model from Odhner et al. (2012), the compliance of the distal finger link was found by considering the variation in energy associated with the perturbation of a point on the distal link. This compliance was characterized at some point  $x$  by a  $6 \times 6$  matrix,  $\mathbf{C}$ , relating a small force  $\delta f$  and a small torque  $\delta \tau$  to a small body-frame displacement  $\delta x$  and body-frame rotation  $\delta \theta$ :

$$\begin{bmatrix} \delta x \\ \delta \theta \end{bmatrix} = \mathbf{C} \begin{bmatrix} \delta f \\ \delta \tau \end{bmatrix} = \begin{bmatrix} \mathbf{C}_{xx} & \mathbf{C}_{x\theta} \\ \mathbf{C}_{x\theta}^T & \mathbf{C}_{\theta\theta} \end{bmatrix} \begin{bmatrix} \delta f \\ \delta \tau \end{bmatrix} \quad (1)$$

The  $3 \times 3$  block matrices  $\mathbf{C}_{xx}$ ,  $\mathbf{C}_{\theta\theta}$ , and  $\mathbf{C}_{x\theta}$  represent the Cartesian and torsional compliance, and the coupling between the two, respectively. At some other point  $x' = x + d$  defined by a rigid-body translation; the Jacobian relating local body-frame motion at  $x'$  to motion at  $x$

is the adjoint operator, which can be written as a  $6 \times 6$  matrix,  $\mathbf{J}$ :

$$\begin{bmatrix} \delta x' \\ \delta \theta' \end{bmatrix} = \mathbf{J} \begin{bmatrix} \delta x \\ \delta \theta \end{bmatrix} = \begin{bmatrix} I^{3 \times 3} & d_x \\ 0 & I^{3 \times 3} \end{bmatrix} \begin{bmatrix} \delta x \\ \delta \theta \end{bmatrix} \quad (2)$$

Here  $I^{3 \times 3}$  is a  $3 \times 3$  identity matrix and  $d_x$  is the  $3 \times 3$  skew-symmetric matrix corresponding to the  $3 \times 1$  vector,  $d$ . The small-force compliance at  $x'$  can also be found using this Jacobian (Salisbury and Craig, 1982):

$$\mathbf{C}' = \mathbf{J} \mathbf{C} \mathbf{J}^T = \begin{bmatrix} I^{3 \times 3} & d_x \\ 0 & I^{3 \times 3} \end{bmatrix} \begin{bmatrix} \mathbf{C}_{xx} & \mathbf{C}_{x\theta} \\ \mathbf{C}_{x\theta}^T & \mathbf{C}_{\theta\theta} \end{bmatrix} \begin{bmatrix} I^{3 \times 3} & 0 \\ d_x^T & I^{3 \times 3} \end{bmatrix} \quad (3)$$

Because (3) describes the compliance of any point on a rigid body given the compliance of a single point, it can be applied to map out the compliance ellipses (which look almost one-dimensional due to the high stiffness in one direction) along the length of the finger. These are plotted in Figure 14 for the iHY finger.

According to these results, the geometry of the distal link is very important to generating an appropriate compliance at the fingertip. Near the distal link's center of compliance, located at a point approximately 6 cm past the base of the distal link, the Cartesian compliance of the fingertip is very small. If the finger were long enough to make contact at this point, the fingertip would resist disturbance forces, but it would also move rigidly, and would not be at all back-driveable due to the stiff actuator tendon. Instead, the finger was shortened so that the finger exhibited significant compliance, principally in the direction normal to the fingertip. To demonstrate that this compliance property is preserved as the finger moves throughout its workspace, the equilibrium configuration of the finger was modeled along its closing trajectory, and the principal fingertip compliance was computed in each configuration (Figure 15). The results of this analysis confirm that the principal direction of compliant motion remains more or less normal to the fingertip as the tendon is contracted. More importantly, the direction of motion of a point on the fingertip is always within approximately 30 degrees of the principal compliance, so that the finger will always deform if the finger is driven into the surface of an object. Thus, proper finger link geometry enables fingertip compliance in the direction of actuation.

The out-of-plane compliance of the fingers, due largely to the torsion of the distal joint flexure (Figure 7), is also critical for producing stable fingertip grasps. The fingers on the SDM Hand were optimized for power grasps, and performed poorly when used for fingertip grasps. The same analysis used to determine in-plane compliance also explains out-of-plane compliance. One important implication of Equation (3) is that the Cartesian compliance at any point on a rigid structure will vary as the square of the translational offset multiplied by the torsional compliance matrix:

$$\mathbf{C}'_{xx} = \mathbf{C}_{xx} + d_x \mathbf{C}_{x\theta}^T + \mathbf{C}_{x\theta} d_x^T + d_x \mathbf{C}_{\theta\theta} d_x^T \quad (4)$$

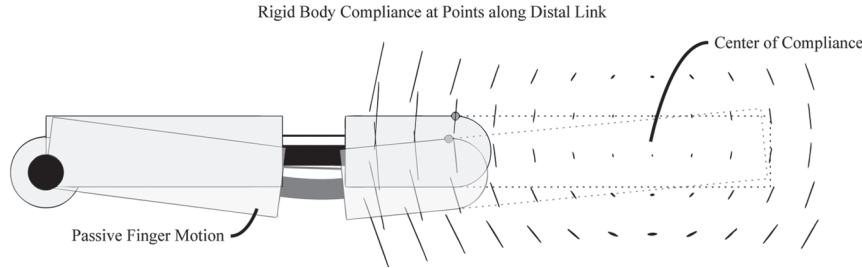


**Fig. 14.** The in-plane compliance of the finger is minimized at its center of compliance. The distal link design was shortened so that contact will occur at a point where there is compliance normal to the fingertip surface, and parallel to the direction of fingertip motion.

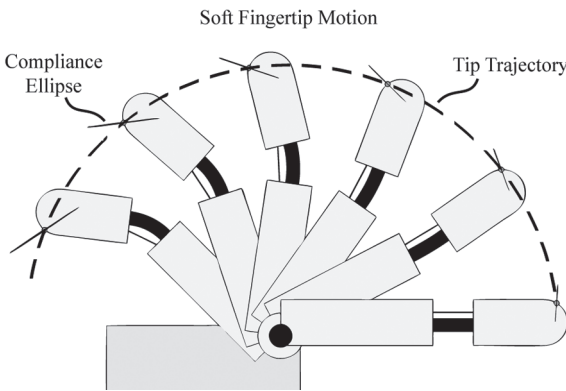


**Fig. 15.** The principal direction of compliance at a point on the tip of the finger, as the finger is moved through its range of motion. The principal direction of compliance is mostly aligned with the direction of motion.

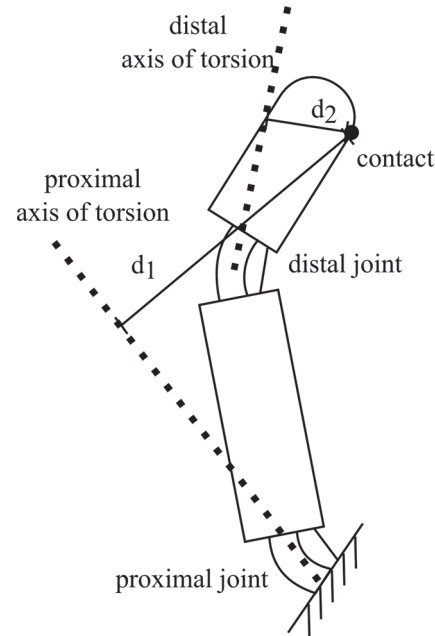


**Fig. 16.** With a flexure at the proximal joint as in the SDM Hand, the proximal joint produces greater Cartesian compliance at the fingertip contact than the distal joint.

The length-squared compliance term,  $d_x \mathbf{C}_{\theta\theta} d_x^T$ , means that the torsional compliance of the proximal joint will produce much more Cartesian compliance at the fingertip than the distal joint, because the moment arm from the fingertip to the axis of out-of-plane joint torsion is longer, as shown in Figure 16. To compensate for this, the proximal joint, originally a flexure in the SDM Hand design, was replaced with a pin joint to increase torsional stiffness in out-of-plane motion. The distal joint, now the dominant source of torsional compliance, was adjusted experimentally to tune the out-of-plane fingertip compliance such that it provided useful compliance during grasp acquisition (e.g. conforming to a tabletop surface), but was stiff enough to enable stable fingertip grasps.

The effect of compliance in fingertip grasps was measured using the same apparatus used to measure the force–excursion curve of a power grasp (Figures 11 and 12). The instrumented cylindrical object was placed between the fingertips, as shown in Figure 17, and the force was measured as the flexor tendons on both fingers were contracted. The increase in contact force plotted in Figure 18 as a function of the tendon excursion is gradual and linear, confirming that the fingertip behaves as a series elastic actuator. The linearity of the fingers is interrupted only at the point when the distal link reaches its travel limit, making contact with

the proximal link. Because this adds an internal constraint on finger motion, the force–excursion relationship stiffens past this point, and still remains predictable.

### 3.3. Fingertip grasp stiffness

In addition to the fingertip force profiles, the stiffness of the iHY Hand was also measured empirically, for opposed pinch grasps and spherical pinch grasps, as illustrated in Figure 3. The measurement apparatus consists of a cylindrical test object 65 mm in diameter attached to a six-axis force/torque sensor (Gamma, by ATI Industrial Automation, Apex, NC, USA). This was mounted in the headstock of a three-axis milling machine, as shown in Figure 19. The hand was held in the milling vise and commanded to grasp the test object. Disturbance displacements were applied to the object using the bed translation of the milling

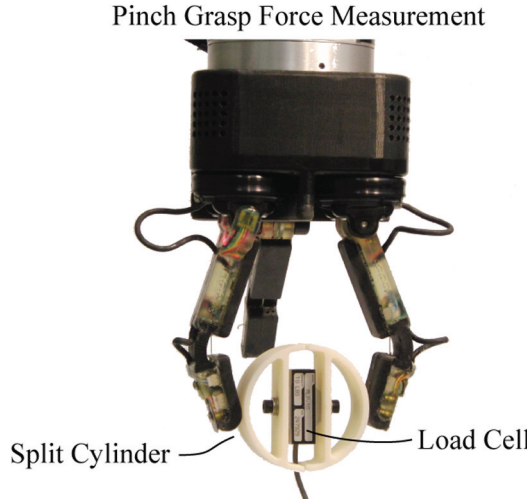


**Fig. 17.** The test apparatus used to measure the force–excursion curve on a 65 mm object in a pinch grasp.

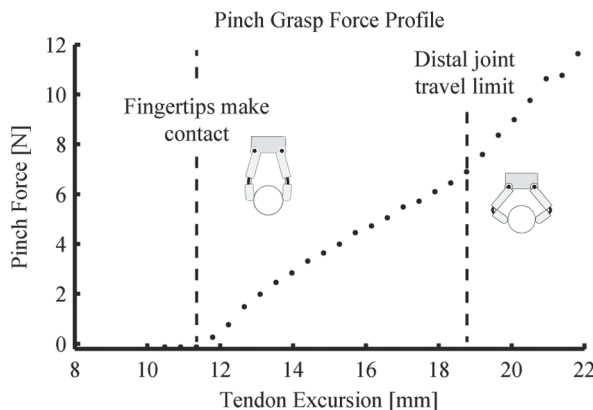


**Fig. 18.** The pinch force on a 65 mm wide object increases gradually and linearly as the tendons are contracted.

machine, and the resultant force was measured. This procedure was performed for a planar fingertip grasp of two opposed fingers, and a spherical fingertip grasp with all three fingers.

An example of the resulting data set is shown in Figure 20. Some hysteresis was observed due to tendon friction and the viscoelasticity of the polymer pads and flexures, and this was dealt with by moving the test object in cycles to obtain an average of the stiffness over both directions of motion. Linear least squares estimation was used to fit the parameters of a symmetric stiffness matrix to the data for both the opposed and spherical fingertip grasps. The estimated stiffness of the two-fingered opposed pinch, in units of N/mm, was

$$\begin{bmatrix} K_{xx} & K_{xy} \\ K_{yx} & K_{yy} \end{bmatrix} \approx \begin{bmatrix} 0.445 & 0.0543 \\ 0.0543 & 0.409 \end{bmatrix} \quad (5)$$

3 Axis Mill Experiment for Measuring Pinch Grasp Stiffness

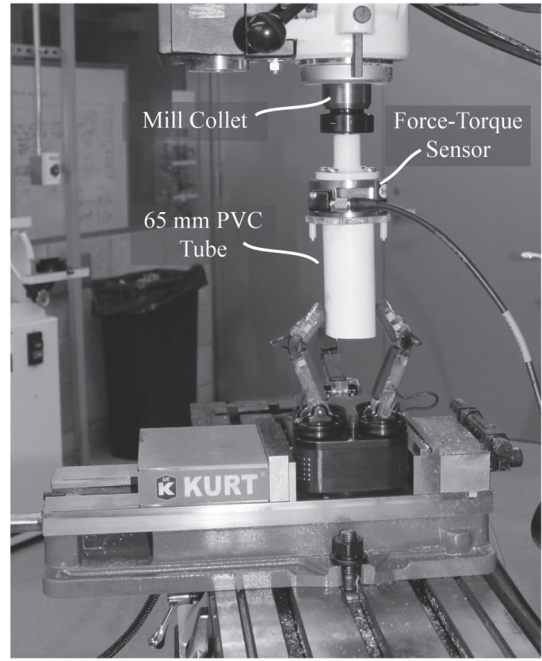


**Fig. 19.** Apparatus for measuring the compliance of planar and spherical pinch grasps. A six-axis force–torque sensor held in a mill headstock is used to measure the force resulting from a rigid displacement in the grasp.

The estimated 3D Cartesian stiffness matrix of the spherical fingertip grasp was

$$\begin{bmatrix} K_{xx} & K_{xy} & K_{xz} \\ K_{yx} & K_{yy} & K_{yz} \\ K_{zx} & K_{zy} & K_{zz} \end{bmatrix} \approx \begin{bmatrix} 0.569 & 0.0553 & 0.0323 \\ 0.0553 & 0.696 & 0.0755 \\ 0.0323 & 0.0755 & 0.809 \end{bmatrix} \quad (6)$$

In each of these results, the stiffness matrix was found to be well-conditioned, having no dominant diagonal terms and consequently no directions of atypically high or low compliance. The magnitude of the measured stiffness can be pictured by envisioning an apple weighing approximately 100 g, causing a deflection of approximately 2 mm for a stiffness of 0.5 N/mm. Therefore, although some deformation will be anticipated due to the weight of grasped objects or contact forces, any small or medium household object will not exceed the fingertip grasping capabilities of the iHY Hand, despite its intrinsic compliance.

### 3.4. Summary

This section has shown how the fingers of the iHY Hand were designed to satisfy two functional requirements: preserving the robust, adaptive power grasping capabilities of the SDM Hand and similar adaptive hands, while adding the ability to grasp with the fingertips as if they were driven by low-impedance actuators. Due to the unique impedance tuning of these fingers, no ad hoc mechanism was needed

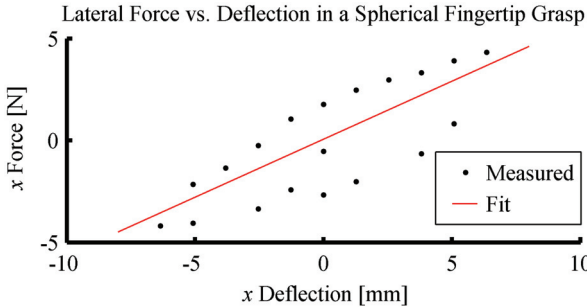


**Fig. 20.** A plot of the force versus deflection for a cyclic position disturbance on an object in a spherical fingertip grasp. The hysteresis observed is due to viscoelasticity in the elastomer pads and flexures, and friction in the tendon sheath.

to enable fingertip grasping, only the adjustment of the finger link lengths relative to the finger's center of compliance and the stiffening of the proximal joint in torsion. Measured force–excursion curves showed that the effect of the passive elasticity on power grasping and fingertip tasks results in a predictable, mostly linear relationship between contact force and tendon excursion.

#### 4. Task performance demonstrations

To show how the design features of the iHY Hand impact its behavior, a series of real-world grasping and manipulation tasks was performed. These tasks included basic pinch and power grasp acquisition, operating tools with triggers, finger pivoting, and transitioning between two- and three-fingertip grasps. This section highlights the design features illustrated by each experiment, and explains how the features of the hand described in Sections 2 and 3 are used in practice. A video from the demonstrations is included with this paper as Multimedia Extension 1.

##### 4.1. Stable passively adaptive grasps

To demonstrate the stability of grasps made with the iHY Hand, Multimedia Extension 1 shows examples of various common grasps executed under teleoperated control. The video segment from 0:20 to 0:50 depicts the acquisition of spherical and cylindrical power grasps on a 230 mm diameter basketball, an irregular, rock-shaped object, and a 153 mm diameter piece of polyvinyl chloride (PVC) pipe. The classic sweeping, then caging behavior described in Section 3.1 can be observed in these grasps. Each of these grasps is stable using only position control on the flexor tendons of the hand. From 0:50 to 1:30, a series of pinch grasps is executed, first a three-finger cylindrical pinch grasp on a telephone receiver, then a battery, a pair of tweezers, and a drill bit. Pinch grasps using the fingernails are demonstrated on small objects including a ball bearing, a key, and a transit card from 1:30 to 2:00. In these clips, no fingertip force

sensing is needed to obtain a stable grasp. It is also interesting to note that the force exerted by the fingertips can be finely adjusted to actuate the tweezers while holding them.

Passive grasp adaptation also simplifies the performance of tasks with position constraints, such as unscrewing the lid of a bottle (Multimedia Extension 1, 2:00). In this example the lid is held in a spherical pinch grasp and the center of rotation of the hand is misaligned with the axis of the bottle. Nevertheless, the finger compliance creates a mechanical coupling that makes it possible to keep a firm grasp of the lid while the lid is tightened or loosened. Similarly, compliance makes it simpler to hold tools in contact with rigid surfaces; the fingertip compliance reduces the precision required of the arm controller and the surface-perceiving system. The sequence from 1:17 to 1:30, showing the grasping of a drill bit and its insertion in a chuck, is a good example of using fingertip compliance to robustly adapt to passive environmental constraints.

The combination of finger durability and compliant adaptability enables apparently complex grasping using very simple control strategies. To demonstrate this, a very basic autonomous system for obtaining objects in a cylindrical pinch grasp is shown in Figure 19. This task was implemented using a calibrated Microsoft Kinect sensor to acquire the centroid and principal axis of a series of objects placed on a table. Much like the experiments performed by the SDM Hand in Dollar and Howe (2010), the iHY Hand was capable of grasping each object simply by moving the center of the palm to the centroid of the object, orienting the fingers along the principal axis of the object, and then closing the fingers on a single pre-recorded trajectory. Figure 21(c) shows a set of objects grasped during this task. Of these, all but the ballpoint pen were grasped successfully greater than 19 of 20 attempts. The small size of the pen led to large errors in the point cloud, so pre-positioning of the hand was less accurate. For this object, 12 of 20 attempts were successful.

Video of a similar autonomous power grasp acquisition experiment is included in Multimedia Extension 1 from 3:20 to 3:45. In this experiment, an earlier printed prototype of the iHY Hand is used in a fashion identical to the pinch grasp process illustrated in Figure 21, but the fingers are driven further into the surface of the table while driving the fingers closed on a feed-forward motion profile, including a small amount of oscillation. This oscillation serves to break the no-slip contact between each finger as the hand closes, so that the fingers can transition from an initial fingertip contact into an enveloping grasp.

##### 4.2. Collision handling with compliance

Several of the demonstrations shown in Multimedia Extension 1 involve incidental or intentional contact of the fingers with the environment, most frequently the tabletop. No active compensation is needed to handle this collision, nor is collision avoided out of a concern for safety.

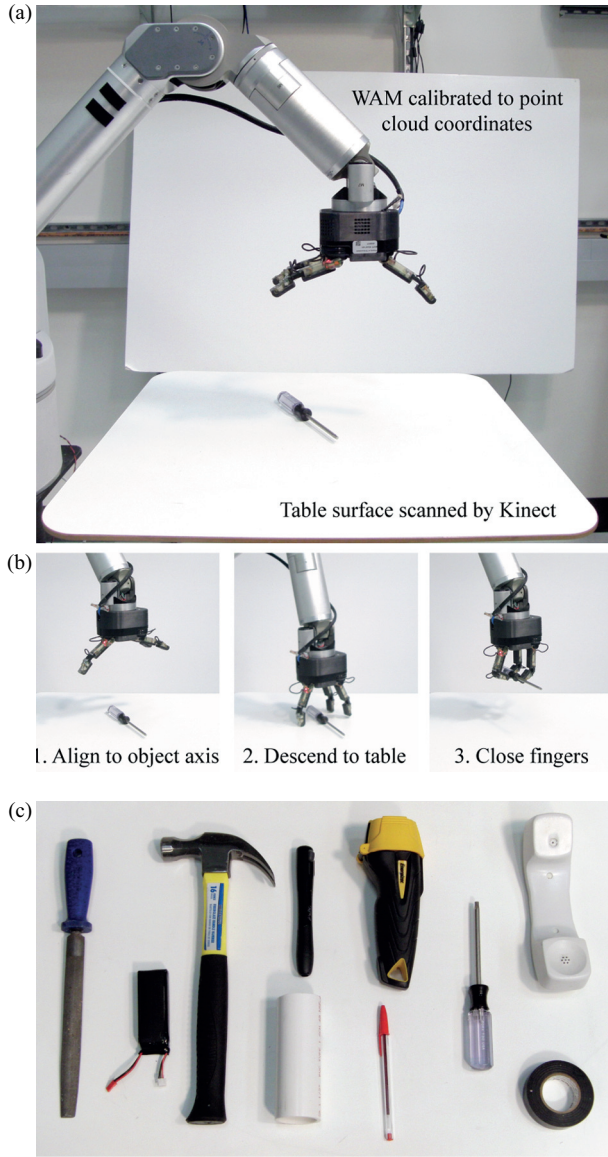


**Fig. 21.** ((a) and (b)) Grasp acquisition task performed autonomously using an overhead Kinect sensor, moving the hand to the centroid of the object, aligning with the major axis, and grasping. (b) Objects grasped during this experiment. WAM: whole arm manipulator.

The passive compliance of the iHY fingers guarantees that the fingers can deform both in bending and in torsion, as depicted in Figure 22 and in Multimedia Extension 1 at 3:08. Objects held in a pinch grasp, in particular, exhibit enough compliance that a grasp can be maintained even if an object experiences significant deflection due to contact, such as the video clip of the battery held in a tripod grasp at 2:08. The ability to safely collide with the environment also allows the hand to safely interact in the immediate vicinity of support surfaces to grasp small objects, even under noisy sensing. Grasping small objects

on a surface, for example, requires either detailed knowledge of the surface's location, or a compliant hand that can simply slide its fingertips along the surface until contact with the object is made, as in the flip-and-pinch tasks shown at 2:48 and described in greater detail by Odhner et al. (2013).

#### 4.3. Variable distal joint stiffness

The flexures in the distal joints of the fingers facilitate passive adaptation of the fingertips to the object geometry. Nevertheless, in some tasks the torsional stiffness of these flexures must be increased such that larger forces can be applied to the object. One of these tasks is turning a key in a lock, where large moments must be applied to the key to perform the task. In this case the key is held in a pinch grasp and the torsional stiffness of the finger is increased by flexing the distal link towards its travel limit, greatly increasing the stiffness of the distal link (Figure 23). Multimedia Extension 1 includes a video of this process at 2:18.

#### 4.4. Finger pivoting and pinch grasp transitions

The set of in-hand manipulation primitives implemented on the iHY Hand are illustrated in Multimedia Extension 1 (2:30). We have shown in previously published work how a hand with the geometry of the planar opposed finger pair can be utilized to perform precision manipulation of an object grasped in a fingertip grasp (Odhner et al., 2012), and to reorient thin objects on flat surfaces repeatedly for pinch grasping (Odhner et al., 2013). The battery shown in Figure 24 and in the video clip was picked up using an opposed pinch grasp and afterward rotated and transitioned to a firmer spherical pinch grasp. During the transition between the grasps the fingertips adjust passively to the battery surface, while maintaining grasping forces as the base of the fingers rotate into the new position.

## 5. Conclusions

The field of robotics is rapidly approaching the long-term goal of fully integrated robots that can sense, perceive, plan, and execute complex tasks in real-world environments. In order for this trend to be truly revolutionary, robot hardware must be widely available, durable enough to survive unplanned collisions, and cheap and easy to repair so that aggressive experimental risks can be taken affordably. The iHY Hand was designed to meet this need through the bottom-up approach, by incrementally extending the functionality of simple hands to encompass a larger set of task objectives as cheaply as possible with minimal added hardware. Sensing was added through the novel repurposing of inexpensive commercial MEMS devices, and additional grasping and manipulation capabilities were added through the novel parameter tuning of the SDM Hand's two-link underactuated fingers rather than the addition of new mechanisms. Non-backdriveable actuators were used

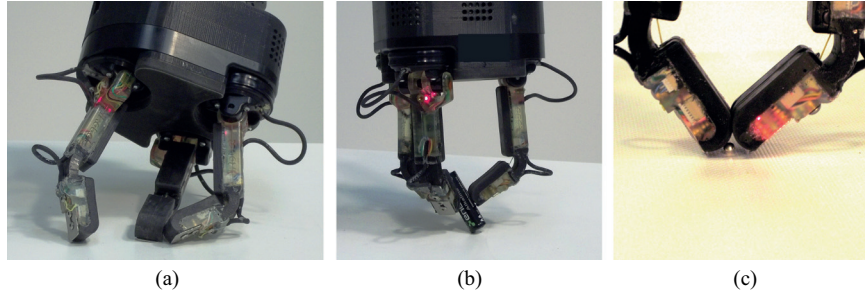


**Fig. 22.** Compliance during tasks; hand is undamaged during unintentional contact with a surface (a), grasped objects are not ejected when they contact environmental obstacles (b), and fingertip operations can be safely performed in contact with obstacles such as table surfaces (c).

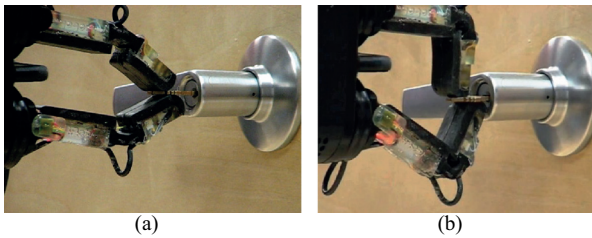


**Fig. 23.** Key insertion/turning task. The key is held in an opposed pinch grasp (a) and then the torsional stiffness of the flexure is increased by bringing the two links into contact at the distal joint.

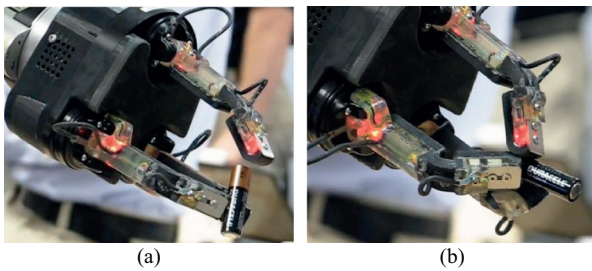


**Fig. 24.** Holding the battery in an opposed pinch grasp (a), and transitioning into the spherical pinch grasp (b) while maintaining grasp forces on the object.

to keep steady-state power usage low, and selective compliance was designed into the hand to ensure that delicate fingertip grasps could still be achieved.

Presently, several dozen iHY Hands have been distributed for use in various research programs. Future designs based on the iHY Hand will focus on further simplifying the chassis, actuators and sensors to further reduce cost and enable wider distribution to end users. Work will also continue on expanding the range of designed-in hand capabilities that can be achieved without the addition of overly complex mechanisms. Finally, there is a great deal of room for growth in the area of sensing, planning, and control of simplified hands performing moderately complex tasks.

## Acknowledgements

The authors would like to thank Frank Hammond from the BioRobotics Laboratory at Harvard University, and Erik Steltz, Wes Huang, and Ben Axelrod at iRobot Corporation for their contributions and insights on the design of the iHY Hand.

## Funding

This work was supported by the DARPA Autonomous Robotic Manipulation program, hardware track (ARM-H; grant number W91CRB-10-C-0141).

## References

- Arai H and Tachi S (1991) Position control of a manipulator with passive joints using dynamic coupling. *IEEE Transactions on Robotics and Automation* 7(4): 528–534.
- Aukes D, et al. (2012) Selectively compliant underactuated hand for mobile manipulation. In: *2012 IEEE International conference on robotics and automation (ICRA)*.
- Begoc V, Krut S, Dombre E, et al. (2007) Mechanical design of a new pneumatically driven underactuated hand. In: *proceedings of the International conference on robotics and automation*, April, pp.927–933.
- Belter JT, Segil J, Dollar AM, et al. (2013) The mechanical design and performance specifications of anthropomorphic prosthetic hands. *Journal of Rehabilitation and Development* 50(5): 599–618.
- Bicchi A and Kumar V (2000) Robotic grasping and contact: A review. In: *proceedings of the IEEE International conference on robotics and automation, 2000 (ICRA'00)*, Vol. 1.
- Bicchi A and Marigo A (2002) Dexterous grippers: Putting non-holonomy to work for fine manipulation. *The International Journal of Robotics Research* 21(5–6): 427–442.
- Birglen L, Laliberté T and Gosselin C (2008) Design and control of the laval underactuated hands. In: *Underactuated Robotic Hands*. Berlin Heidelberg: Springer, pp. 171–207.
- Bridgewater LB, et al. (2012) The Robonaut 2 hand-designed to do work with tools. In: *2012 IEEE International conference on robotics and automation (ICRA)*.
- Cham JG, et al. (1999) Layered manufacturing with embedded components: Process planning considerations. In: *proceedings of the 1999 ASME DETC/DFM conference*.

- Chu J-u, Jung D and Lee Y (2008) Design and control of a multi-function myoelectric hand with new adaptive grasping and self-locking mechanisms. In: *2008 IEEE International conference on robotics and automation*, May, pp.743–748.
- Ciocarlie M, Hicks F and Stanford S (2013) Kinetic and dimensional optimization for a tendon-driven gripper. In: *IEEE International conference on robotics and automation*.
- Crisman JD, Kanojia C and Zeid I (1996) Graspar: A flexible, easily controllable robotic hand. *IEEE Robotics & Automation Magazine* 3(2): 32–38.
- Cutkosky MR (1989) On grasp choice, grasp models, and the design of hands for manufacturing tasks. *IEEE Transactions on Robotics and Automation* 5(3): 269–279.
- Dahiya RS, et al. (2007) POSFET based tactile sensor arrays. In: *14th IEEE International conference on electronics, circuits and systems, 2007 (ICECS 2007)*.
- Dollar AM and Howe RD (2006) A robust compliant grasper via shape deposition manufacturing. *IEEE/ASME Transactions on Mechatronics* 11(2): 154–161.
- Dollar AM and Howe RD (2010) The highly adaptive SDM hand: Design and performance evaluation. *International Journal of Robotics Research* 29(5): 585–597.
- Grebenstein M, et al. (2012) The hand of the DLR hand arm system: Designed for interaction. *The International Journal of Robotics Research* 31(13): 1531–1555.
- Grioli G, Catalano M, Silvestro E, et al. (2012) Adaptive synergies: An approach to the design of under-actuated robotic hands. In: *2012 IEEE/RSJ International conference on intelligent robots and systems (IROS)*, pp.1251–1256.
- Hanafusa H and Asada H (1977) Stable prehension by a robot hand with elastic fingers. In: *proceedings of the 7th International symposium on industrial robots*.
- Hirose S and Umetani Y (1978) The development of soft gripper for the versatile robot hand. *Mechanism and Machine Theory* 13(3): 351–359.
- Jacobsen S, et al. (1986) Design of the Utah/MIT dexterous hand. In: *proceedings of the 1986 IEEE International conference on robotics and automation*, Vol. 3.
- Jentoft LP and Howe RD. (2011) Determining object geometry with compliance and simple sensors. In: *2011 IEEE/RSJ International conference on intelligent robots and systems (IROS)*.
- Jentoft LP and Howe RD (2012) Force sensing with compliant joints workshop: advances in tactile sensing and touch-based human-robot interaction. In: *human robot interaction 2012*, Boston, MA, 5–8 March.
- Kinova Robotics (2013) JACO. Available at: <http://www.kinovarobotics.com/products/jaco-research-edition/> (accessed 26 November 2013).
- Kragten G, et al. (2011) Stable precision grasps by underactuated grippers. *IEEE Transactions on Robotics* 27(6): 1056–1066.
- Kuka YouBot (2013) Available at: <http://www.youbot-store.com/ybproductinfo.aspx> (accessed 26 November 2013).
- Mason MT, Rodriguez A, Srinivasa SS, et al. (2012) Autonomous manipulation with a general-purpose simple hand. *The International Journal of Robotics Research* 31(5): 688–703.
- Matheus K and Dollar AM (2010) Benchmarking grasping and manipulation: Properties of the objects of daily living. In: *2010 IEEE/RSJ international conference on intelligent robots and systems (IROS)*.
- Merz R, et al. (1994) Shape deposition manufacturing. In: *proceedings of the solid freeform fabrication symposium 1994*, Austin, TX, USA, pp. 1–8.
- Nagata K (1994) Manipulation by a parallel-jaw gripper having a turntable at each fingertip. In: *proceedings of the International conference on robotics and automation*. IEEE.
- Odhner LU and Dollar AM (2012) The smooth curvature model: An efficient representation of Euler-Bernoulli flexures as robot joints. *IEEE Transactions on Robotics* 28(4): 761–772.
- Odhner LU, Ma RR and Dollar AM (2012) Experiments in underactuated in-hand manipulation. In: *proceedings of the international symposium on experimental robotics*, 17–21 June, Quebec City, Canada.
- Odhner LU, Ma RR and Dollar AM (2013) Open-loop precision grasping with underactuated hands inspired by a human manipulation strategy. *IEEE Transactions on Automation Science and Engineering* 10(3): 625–633.
- Okada T (1979) Object-handling system for manual industry. *IEEE Transactions on Systems, Man and Cybernetics* 9(2): 79–89.
- Okamura AM, Smaby N and Cutkosky MR (2000) An overview of dexterous manipulation. 2000. In: *proceedings of the IEEE International conference on robotics and automation (ICRA'00)*, vol. 1.
- Pratt GA and Williamson MM (1995) Series elastic actuators. In: *proceedings of the IEEE International conference on intelligent robots and systems*, vol. 1, pp.399–406.
- Quenouelle C and Gosselin C (2009) A quasi-static model for planar compliant parallel mechanisms. *ASME Journal of Mechanisms and Robotics* 1(2).
- Resnik L, et al. (2013) Development and evaluation of the activities measure for upper limb amputees. *Archives of Physical Medicine and Rehabilitation* 24(3): 488–494.
- Robotiq (2013) 3-finger adaptive robot gripper. Available at: <http://www.robotiq.com/en/products/industrial-robot-hand/> (accessed 26 November 2013).
- Roy B and Asada HH (2009). Nonlinear feedback control of a gravity-assisted underactuated manipulator with application to aircraft assembly. *IEEE Transactions on Robotics* 25(5): 1125–1133.
- Rus D (1992) Dexterous rotations of polyhedra. In: *proceedings of the 1992 IEEE International conference on robotics and automation*.
- Saliba M and de Silva C (1991) An innovative robotic gripper for grasping and handling research. In: *proceedings of IECON '91*, pp. 975–979.
- Salisbury JK and Craig J (1982) Articulated hands force control and kinematic issues. *The International Journal of Robotics Research* 1(1): 4–17.
- Schmitz A, Pattacini U, Nori F, et al. (2010) Design, realization and sensorization of the dexterous iCub hand. In: *2010 10th IEEE-RAS international conference on humanoid robots (humanoids)*, December, pp. 186–191.
- Schunk Robotic Hands SDH (2013) Available at: <http://www.schunk-modular-robotics.com/left-navigation/service-robotics/components/actuators/robotic-hands/sdh.html> (accessed 26 November 2013).
- Takaki T and Omata T (2006) 100g-100N finger joint with load-sensitive continuously variable transmission. In: *proceedings of the International conference on robotics and automation*, pp. 976–981.

- Tenzer Y, Jentoft LP and Howe RD (2012) Inexpensive and easily customized tactile sensors using MEMS barometers chips. *IEEE Robotics and Automation Magazine* (conditionally accepted)
- The Shadow Robot Company (2013) Shadow dexterous hand. Available at: <http://www.shadowrobot.com/products/dexterous-hand> (accessed 26 November 2013).
- Tincani V, Catalano MG, Farnioli E, et al. (2012) Velvet fingers: a dexterous gripper with active surfaces. In: *Intelligent robots and systems (IROS), 2012 IEEE/RSJ International conference on*, Vilamoura, Portugal, 7–12 October 2012. IEEE.
- Ulrich N, Paul R and Bajcsy R (1988) A medium-complexity compliant end effector. In: *proceedings of the 1988 IEEE International conference on robotics and automation*, April, pp.434–436.
- Willow Garage (2013) PR2. Available at: <http://www.willowgarage.com/pages/pr2/overview/> (accessed 26 November 2013).
- Yoshikawa T (1985) Manipulability of robotic mechanisms. *The International Journal of Robotics Research* 4(2): 3–9.

## Appendix: Index to Multimedia Extensions

The Multimedia extension page is found at <http://www.ijrr.org>

**Table of Multimedia Extensions**

Extension	Type	Description
1	Video	This video demonstrated the performance of the iHY hand performing the grasp primitives it was designed around including (1) robust power grasps, (2) stable pinch grasps, (3) regrasping and reorientation.